

# Phosphorus-Doped Ordered Mesoporous Carbons with Different Lengths as Efficient Metal-Free Electrocatalysts for Oxygen Reduction Reaction in Alkaline Media

Dae-Soo Yang, Dhruvajyoti Bhattacharjya, Shaukatali Inamdar, Jinsol Park, and Jong-Sung Yu\*

Department of Advanced Materials Chemistry, Korea University, 2511 Sejong-ro, Sejong 339-700, Republic of Korea

**S** Supporting Information

**ABSTRACT:** Phosphorus-doped ordered mesoporous carbons (POMCs) with different lengths were synthesized using a metal-free nanocasting method of SBA-15 mesoporous silica with different sizes as template and triphenylphosphine and phenol as phosphorus and carbon sources, respectively. The resultant POMC with a small amount of P doping is demonstrated as a metal-free electrode with excellent electrocatalytic activity for oxygen reduction reaction (ORR), coupled with much enhanced stability and alcohol tolerance compared to those of platinum via four-electron pathway in alkaline medium. Interestingly, the POMC with short channel length is found to have superior electrochemical performances compared to those with longer sizes.

Energy is one of the biggest challenges for the 21st century. There has been an ever increasing demand for environmental friendly high-power energy sources. Fuel cells (FCs) are envisioned as one of the best possible solutions due to their high energy density, high efficiency, and negligible emission of harmful gases. The foremost limitation in low-temperature FCs is the kinetically sluggish oxygen reduction reaction (ORR) at the cathode, which necessitates the use of a substantial amount of catalyst. To date the best materials for catalysis of ORR are platinum (Pt) and its alloys.<sup>1</sup> However, despite the considerable research efforts in Pt-based FCs, large-scale commercialization is still restricted mainly by slow electron-transfer kinetics (particularly at the cathode<sup>2</sup>), high cost, poor durability, and shortage of the noble metal. As a result, the global research efforts were directed toward the search for broad-range alternative catalysts based on non-precious metals,<sup>2</sup> their alloys or oxides,<sup>3</sup> nitrogen-coordinated metal,<sup>4</sup> and metal-free doped carbon.<sup>5</sup> Metal or metal oxide catalysts frequently suffer from dissolution, sintering, and agglomeration during fuel cell operation which can reduce activity and durability.<sup>6</sup> This problem can be addressed by using metal-free doped carbon materials. Among the doped carbon materials, N-doping has been the most popular choice.<sup>6</sup> N-doped carbon nanotubes,<sup>7</sup> ordered mesoporous graphitic arrays,<sup>8</sup> nanoshell carbons,<sup>9</sup> and graphene sheets<sup>10</sup> have been shown to exhibit high electrocatalytic activities for ORR. The introduction of heteroatoms in carbonaceous supports has also been reported to improve the performance of ORR electrocatalysts including platinum-group metals.<sup>1c,d</sup> When a heteroatom is bonded with a carbon framework, it introduces a defect in the nearby sites due to

difference in bond length and atomic size, and thereby can induce uneven charge distribution.<sup>11</sup> Furthermore, since the heteroatom is usually covalently bonded within a carbon framework, its effect will not fade even for long-time operation. In fact, N-doped carbon materials have shown better durability than that of commercial Pt/VC catalysts.<sup>11</sup> These properties encouraged researchers to explore doping of carbon materials with other heteroatoms such as boron,<sup>12</sup> phosphorus,<sup>13</sup> and iodine.<sup>14</sup> Especially, the first phosphorus-doped graphitic layers and MCNTs are reported to show high electrocatalytic performance by Peng and co-workers.<sup>13</sup> Phosphorus–nitrogen dual-doped carbon was also reported recently.<sup>15</sup>

Phosphorus has the same number of valence electrons as nitrogen and often shows similar chemical properties; however, it has a larger atomic radius and higher electron-donating ability which make it an astute choice as a dopant to carbon materials and thus is expected to enhance the catalytic activity as well. Despite these possible advantages of phosphorus and the requirement of novel materials with a high electroactive surface area for high performance, there has been no report for development of a possible blend of phosphorus and large surface area possessing carbon material to improve catalytic activity and durability. Ordered mesoporous carbons (OMCs) have been a popular choice as electrocatalyst supports for fuel cells<sup>16</sup> because of their high surface area, tunable pore size, and large pore volume with narrow pore size distributions, allowing facile molecular transport of reactants and products.<sup>17</sup> Doping of the OMC by a phosphorus heteroatom can produce an excellent blend that can be very effective for largely enhancing its electrocatalytic activity.

In this communication, we demonstrate the novel phosphorus-doped ordered mesoporous carbon (POMC) as a very efficient electrocatalyst for ORR in alkaline media. The POMCs were synthesized by copyrolyzing a phosphorus-containing source and a carbon source using SBA-15 ordered mesoporous silica as a template without the use of any metal components, which can intrinsically avoid involvement of any metal components in electrocatalytic activity, elucidating only the effect of P in the carbon framework. Electrocatalytic performances of the prepared novel POMC materials have exhibited not only excellent catalytic activity for ORR in alkaline medium but also much better tolerance for methanol oxidation and much higher stability than commercial, state-of-

Received: June 30, 2012

Published: September 11, 2012

the-art Pt/C catalysts. We have also successfully elucidated the effect of the mesopore channel length of a POMC on the electrocatalytic performance.

A schematic illustration of the fabrication process of POMC is shown in Figure 1a, further details of which can be found in

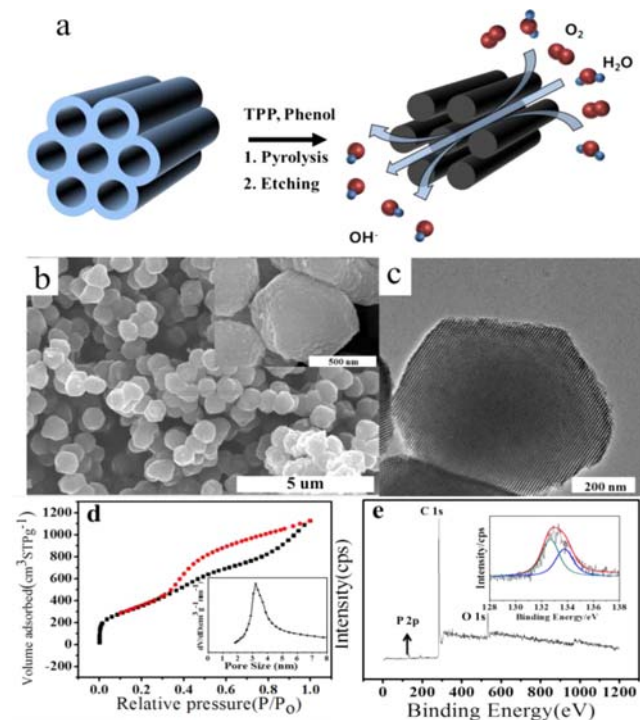


**Figure 1.** (a) Schematic illustration of POMC preparation, (b) FE-SEM image with an inset showing magnified image of POMC-3, (c) TEM image, (d)  $N_2$  sorption isotherms with an inset showing pore size distribution and (e) XPS survey scan and P 2p spectrum of POMC-3.

Supporting Information (SI). Briefly, a mixture of a phosphorus-containing carbon source, triphenylphosphine (TPP), and a primary carbon precursor (phenol) was infiltrated into a SBA-15 template at room temperature and pyrolyzed at 900 °C in an argon environment followed by removal of the template by HF etching to get silica-free POMC. Three differently sized POMCs were prepared by altering the SBA-15 templates with different rod lengths.<sup>18</sup> The obtained POMCs with different lengths were designated as POMC-1, POMC-2, and POMC-3 in decreasing order in length of 1.5, 1.0, and 0.7  $\mu\text{m}$  with thicknesses of 0.2, 0.4, and 0.6  $\mu\text{m}$ , respectively.

The structure and morphologies of the synthesized POMC were characterized by FE-SEM and TEM measurements. The FE-SEM image of POMC-3 reveals the formation of a uniform distribution of nearly spherical carbon microstructures with average length and thickness of about 0.7 and 0.6  $\mu\text{m}$ , respectively, as illustrated in Figure 1b. The formation of highly ordered uniform pore distribution can be seen in the TEM image of POMC-3 in Figure 1c. The surface area and pore size of the synthesized POMC were determined by  $N_2$  adsorption–desorption isotherms. The isotherms and pore size distribution (PSD) of POMC-3 are shown in Figure 1d. The PSD was derived to be about 3.4 nm from the analysis of the adsorption branch using the Barrett–Joyner–Halenda (BJH) method. The isotherms of type IV with an H1-type hysteresis loop (characteristic of mesoporous materials having channel-type

pores) were observed for all the samples. All comparative SEM and TEM images along with other surface properties for all the synthesized POMCs with different rod lengths are given in the SI (Figure S1 and Table S1). Brunauer–Emmett–Teller (BET) analysis confirms high surface area mesostructures for the resulting POMC materials with uniform mesopore sizes. The BET surface area increases gradually from 814 to 930 and finally 1182  $\text{m}^2 \text{g}^{-1}$ , while the total pore volume increases from 1.40 to 1.66 and 1.87  $\text{cm}^3 \text{g}^{-1}$  for the POMC-1, POMC-2, and POMC-3, respectively. The amount of phosphorus doping and its nature of bonding with the carbon framework were investigated by X-ray photoelectron spectroscopy (XPS) measurements. The XPS survey spectrum of POMC-3 given in Figure 1e shows a predominant peak at 284.6 eV corresponding to C, and a peak at 532 eV, to O, and peak at 133.3 eV, to P 2p. The high-resolution P 2p XPS spectrum in the inset of Figure 1e reveals the presence of both P–O bonding (133.8 eV) and P–C bonding (132.7 eV) in the prepared POMC-3.<sup>19</sup> The results strongly suggest that the phosphorus atoms are incorporated into the carbon framework of the POMC. Quantitative XPS analysis shows that phosphorus is present with  $\sim 1.36$  atom % in the framework. The P contents of other POMCs with longer length were also determined and are summarized in Table S2 of SI. The values are similar to those determined by energy-dispersive X-ray spectra (Figure S7 and Table S2 in SI).

To investigate the electrocatalytic activity of the P-doped OMC for the ORR, we have performed three-electrode cyclic voltammetry (CV) experiments in  $O_2$ -free and  $O_2$ -saturated solution with 0.1 M KOH at a scan rate of 100  $\text{mV s}^{-1}$ . The results were compared with those of undoped OMC and commercial Pt/VC catalyst (20 wt % Pt supported on Vulcan XC72R carbon (VC) from E-TEK). The corresponding voltammograms can be seen in Figure 2a–c. Figure 2a shows featureless CV within the ORR potential range for the POMC-3 in the  $O_2$  free solution (black color). In contrast, for the electrolyte solution saturated with  $O_2$ , a distinct ORR peak is observed at  $-0.19$  V, which confirms electrocatalytic activity of POMC-3 for oxygen reduction. When the CV of POMC-3 (Figure 2a) was compared with that of undoped OMC (Figure 2b), it is evident that phosphorus doping to OMC has significantly enhanced the ORR current. This is probably due to presence of defect-induced active sites for  $O_2$  adsorption, which are generated by changes in the bond length and the bond angle of the C–P bond. In addition, the available electron pair in phosphorus may enhance asymmetric spin density in adjacent carbon atoms and promote ORR activity.<sup>13</sup> It is well-known that methanol can penetrate through proton exchange membrane and deteriorate cathode Pt catalyst which is a major concern for direct methanol fuel cell. N-doped carbon materials have been shown to be highly selective for ORR even in presence of methanol.<sup>8</sup> To check this ability for POMC, we have also recorded CVs in  $O_2$ -saturated 0.1 M KOH in the presence of 1.0 M methanol and measured the electrocatalytic selectivity of POMCs, undoped OMC, and Pt/VC. For the Pt/VC catalyst, one pair of very strong peaks at  $-0.18$  and  $-0.21$  V was observed for methanol oxidation in the CV curve, whereas the cathodic ORR peak vanished (Figure 2c). In contrast, no noticeable change was observed in the oxygen-reduction current on POMC-3 and undoped OMC under the same conditions. All these results confirm that POMC exhibits high catalytic activity for ORR with an extraordinary selectivity for oxygen to evade crossover effects

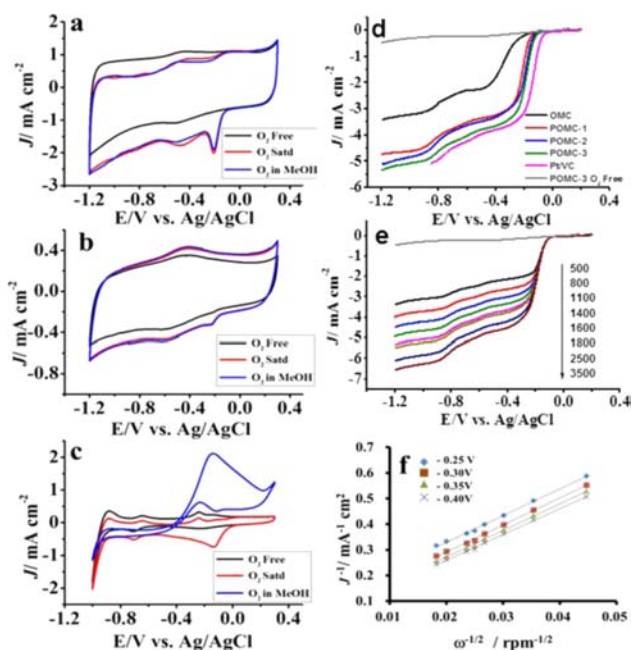


**Figure 2.** CVs for the ORR at  $100 \text{ mV s}^{-1}$  for POMC-3 (a), undoped OMC (b), and commercial Pt (20 wt %)/VC catalyst (c) at different conditions. Also shown are LSV curves for OMC, POMCs of different sizes, and Pt/VC catalyst at 1600 rpm along with  $\text{O}_2$ -free current of POMC-3 (d), LSV curves for POMC-3 at different rotation speeds along with  $\text{O}_2$ -free LSV shown in gray color for comparison (e) on a glassy carbon rotating disk electrode in 0.1 M KOH solution saturated by  $\text{O}_2$  at a scan rate of  $10 \text{ mV s}^{-1}$ , and K-L plots of POMC-3 derived from RDE data at different electrode potentials (f).

of the alcohol and thereby outperforms even the commercial Pt/VC electrode. It can be assessed instantly that our POMC material holds high promise for use as a cathode in direct methanol and alkaline fuel cells. Interestingly, the methanol crossover may be less of a problem in alkaline fuel cells since the  $\text{OH}^-$  anions migrate from the cathode to the anode and, by doing so, can block the methanol crossover from the anode to the cathode.

To better understand the electrocatalytic performance of the POMC catalysts during the ORR process, we compared their electrocatalytic performances with those of undoped OMC and commercial Pt/VC by linear sweep voltammetry (LSV) using a rotating disk electrode (RDE). For RDE voltammetry measurements, the same amount of each catalyst ( $0.79 \text{ mg/cm}^2$ ) was loaded onto a glassy carbon RDE, and LSV was performed in an  $\text{O}_2$ -saturated 0.1 M KOH solution with an  $\text{O}_2$  flow rate of  $20 \text{ mL min}^{-1}$  at a rotation speed of 1600 rpm and a scan rate of  $10 \text{ mV s}^{-1}$ . As shown in Figure 2d, undoped OMC (black line) exhibited an inefficient two-step ORR process with onset potentials at  $-0.23$  and  $-0.62 \text{ V}$ , which are attributable to the reductions of  $\text{O}_2$  to  $\text{HO}_2^-$  and  $\text{HO}_2^-$  to  $\text{OH}^-$ , respectively. Unlike undoped OMC, all of the POMCs demonstrated a one-step process for ORR with a lower onset potential at  $\sim -0.11 \text{ V}$  and a much higher current density.

The effect of the channel length of the prepared POMCs on catalytic ORR performance was also investigated in Figure 2d. Interestingly, the POMCs with different rod lengths also revealed different onset potentials and current densities: the shorter the rod length, the better the ORR performance. To understand the channel-length effect of POMCs on their electrocatalytic performances, electrochemical impedance spec-

troscopy (EIS) was carried out. The Nyquist plots obtained (Figure S6, SI) were compared for the different channel lengths of POMCs. The charge transfer resistance ( $R_{\text{ct}}$ ) values obtained for POMCs were 29.7, 24.1, and  $10.5 \Omega$  for POMC-1, POMC-2, and POMC-3, respectively. Thus, a decrease in channel length lowered the resistance of POMCs, which can ultimately lead to an increase in electrocatalytic activity. Although oxygen molecules with a kinetic diameter of  $0.34 \text{ nm}^{20}$  can penetrate into the mesopore channel ( $\sim 3.2 \text{ nm}$  in diameter) of POMCs with no geometrical hindrance, it is likely that  $\text{O}_2$  molecules have less resistance in shorter channels, which leads to a higher ORR performance compared to that of longer channels. This is in good agreement with the literature, where it was reported that mesoporous carbon with short lengths showed much higher capacitance retention than did the samples with long lengths.<sup>21</sup>

For further insight into electron transfer parameters of the POMC-3 catalyst, the RDE measurements were performed at various rotating speeds and are shown in Figure 2e. As for commercial Pt/VC catalysts, the observed polarization curves for POMC-3 suggest four-electron pathways for reduction of  $\text{O}_2$  to  $\text{OH}^-$  with little to negligible formation of  $\text{HO}_2^-$ . It is well-known that the limited diffusion current densities ( $J_{\text{L}}$ ) depend on the rotation speed ( $\omega$ ) of the RDE, and therefore by using the Koutecky–Levich (K-L) equation on this relationship, the number of electron transfers ( $n$ ) involved in the ORR can be calculated (details of the calculation method are provided in SI). As shown in Figure 2f, the  $n$  value for POMC-3 was calculated to be 3.91 at  $-0.25 \text{ V}$ , which is close to the onset potential for ORR at other electrode potentials, thereby indicating a four-electron transfer reaction. In contrast, undoped OMC has shown an  $n$  value of about 2.4, evidencing a two-electron pathway (Figure S4 in SI). The  $n$  values for all the cathode materials studied are summarized in Table S1 of SI. On the basis of the values of the ORR peak potential and the current density, the activities of the POMCs are found to be higher compared to that of the P-doped graphite reported earlier.<sup>13</sup> The oxygen reduction reaction occurred at  $-0.19$  and  $-0.23 \text{ V}$  for the commercial Pt/C and POMC-3, respectively, in this work. The difference is only  $0.04 \text{ V}$ . In contrast, the difference was  $0.18 \text{ V}$  on the basis of  $-0.19$  and  $-0.37 \text{ V}$  for the oxygen reduction reaction peaks of commercial Pt/C and P-doped graphite, respectively, indicating much faster ORR activity for the POMC compared to that for P-doped graphite.<sup>13a</sup>

Another main challenge in fuel cell applications is durability of electrocatalysts in the electrode. The POMC-3 was also analyzed for durability by running CVs for 4000 cycles, and the results support excellent long-term performance for the prepared POMC, as the activity is almost constant over 4000 cycles in comparison to almost 90% fading of activity in the commercial Pt/VC catalyst (Figure S5 in SI).

In summary, the fabrication of novel P-doped OMC cathodes has been demonstrated by a simple, cost-effective, and readily reproducible metal-free nanocasting approach. The resulting POMC, with a small amount of P doping (less than 1.5 atom %) as the true metal-free catalyst, exhibited outstanding electrocatalytic activity, long-term stability, and excellent resistance to alcohol crossover effects for ORR in alkaline media. The P-doping induces defects in the carbon framework and increases the electron delocalization due to good electron-donating properties of P, promoting active sites for ORR. The effect of channel length of the prepared POMC on catalytic



ORR performance was also investigated, showing an increase in activity with a decrease in the length of the POMC, probably due to increased surface area and decreased resistance of shorter channels. Overall, with proper optimization on the amount of P-loading and distribution, which is now in progress, the future replacement of the expensive Pt/VC catalyst can be achieved by the more stable, effective, and cheap P-doped carbon for practical applications of fuel cells.

## ■ ASSOCIATED CONTENT

### ■ Supporting Information

Experimental and characterization details; SEM and TEM images; BET results; impedance, cycle performance, and EDX data. This material is available free of charge via the Internet at <http://pubs.acs.org>

## ■ AUTHOR INFORMATION

### Corresponding Author

jsyu212@korea.ac.kr

### Notes

The authors declare no competing financial interest.

## ■ ACKNOWLEDGMENTS

This work was supported by NRF Grant (NRF 2010-0029245) and Global Frontier R&D Program on Center for Multiscale Energy System (NRF 2011-0031571) funded by the Ministry of Education, Science and Technology through the National Research Foundation of Korea. We also thank the KBSIs at Jeonju, Chuncheon, and Daejeon for SEM, TEM, and XRD measurements.

## ■ REFERENCES

- (1) (a) Fang, B.; Kim, J. H.; Kim, M.-S.; Yu, J.-S. *Chem. Mater.* **2009**, *21*, 789. (b) Fang, B.; Chaudhari, N. K.; Kim, M. -S.; Kim, J. H.; Yu, J.-S. *J. Am. Chem. Soc.* **2009**, *131*, 15330. (c) Noto, V. D.; Negro, E. *Electrochim. Acta* **2010**, *55*, 7564. (d) Noto, V. D.; Negro, E.; Vezzu, K.; Toniolo, L.; Pace, G. *Electrochim. Acta* **2011**, *57*, 257.
- (2) (a) Kongkanand, A.; Kuwabata, S.; Girishkumar, G.; Kamat, P. *Langmuir* **2006**, *22*, 2392. (b) Zhang, J.; Sasaki, K.; Sutter, E.; Adzic, R. *Science* **2007**, *315*, 220. (c) Lim, B.; Jiang, M. J.; Camargo, P. H. C.; Cho, E. C.; Tao, J.; Lu, X. M.; Zhu, Y. M.; Xia, Y. N. *Science* **2009**, *324*, 1302. (d) Colmati, F.; Antolini, E.; Gonzalez, E. R. *J. Power Sources* **2006**, *157*, 98. (e) Zhang, J.; Yang, H. Z.; Fang, S. J. Y.; Zou, H. *Nano Lett.* **2010**, *10*, 638. (f) Yu, J.-S.; Kim, M.-S.; Kim, J. H. *Phys. Chem. Chem. Phys.* **2010**, *12*, 15274.
- (3) Chen, W.; Kim, J. M.; Sun, S. H.; Chen, S. W. *J. Phys. Chem.* **2008**, *112*, 3891.
- (4) (a) Yu, X.; Ye, S. *J. Power Source* **2007**, *172*, 145. (b) Shao, Y. Y.; Liu, J.; Wang, Y.; Lin, Y. H. *J. Mater. Chem.* **2009**, *19*, 46.
- (5) (a) Gong, K. P.; Du, F.; Xia, Z. H.; Durstock, M.; Dai, L. M. *Science* **2009**, *323*, 760. (b) Tang, Y.; Allen, B. L.; Kauffman, D. R.; Star, A. *J. Am. Chem. Soc.* **2009**, *131*, 13200. (c) Niwa, H.; Horiba, K.; Harada, Y.; Oshima, M.; Ikeda, T.; Terakura, K.; Ozaki, J.; Miyata, S. *J. Power Sources* **2009**, *187*, 93.
- (6) (a) Liu, R. L.; Wu, D. Q.; Feng, X. L.; Mullen, K. *Angew. Chem., Int. Ed.* **2010**, *49*, 2565. (b) Wang, Y. J.; Wilkinson, D. P.; Zhang, J. J. *Chem. Rev.* **2011**, *111*, 7625. (c) Wu, Z. S.; Yang, S.; Yi Sun, Y.; Parvez, K.; Feng, X.; Mullen, K. *J. Am. Chem. Soc.* **2012**, *134*, 9082.
- (7) Xuan, X.; Lijun, Y.; Shujuan, J.; Zheng, H.; Songqin, L. *Chem. Commun.* **2011**, *47*, 7137.
- (8) Liu, R. L.; Wu, D. Q.; Feng, X. L.; Mullen, K. *Angew. Chem., Int. Ed.* **2010**, *49*, 2565.
- (9) Ozaki, J.; Tanifuji, S.; Furuichi, A.; Yabutsuka, K. *Electrochim. Acta* **2010**, *55*, 1864.

(10) (a) Lee, K. R.; Lee, K. U.; Lee, J. W.; Ahn, B. T.; Woo, S. I. *Electrochem. Commun.* **2010**, *12*, 1052. (b) Qu, L. T.; Liu, Y.; Baek, J. B.; Dai, L. M. *ACS Nano* **2010**, *4*, 1321.

(11) (a) Gong, K. P.; Du, F.; Xia, Z. H.; Durstock, M.; Dai, L. M. *Science* **2009**, *323*, 760. (b) Tang, Y.; Allen, B. L.; Kauffman, D. R.; Star, A. *J. Am. Chem. Soc.* **2009**, *131*, 13200. (c) Shao, Y.; Zhang, S.; Engelhard, M. H.; Li, G.; Shao, G.; Wang, Y.; Liu, J.; Aksay, I. A.; Lin, Y. *J. Mater. Chem.* **2010**, *20*, 7491.

(12) Yang, L.; Jiang, S.; Zhao, Y.; Zhu, L.; Chen, S.; Wang, X.; Wu, Q.; Ma, J.; Ma, Y.; Hu, Z. *Angew. Chem., Int. Ed.* **2011**, *50*, 7132.

(13) (a) Liu, Z. W.; Peng, F.; Wang, H. J.; Yu, H.; Zheng, W. X.; Yang, J. *Angew. Chem., Int. Ed.* **2011**, *50*, 3257. (b) Liu, Z. W.; Peng, F.; Wang, H.; Yu, H.; Tan, J.; Zhu, L. *Catal. Commun.* **2011**, *16*, 35.

(14) Yao, Z.; Nie, H.; Yang, Z.; Zhou, X.; Liu, Z.; Huang, S. *Chem. Commun.* **2012**, *48*, 1027.

(15) (a) Deak, D. V.; Biddinger, E. J.; Luthman, K. A.; Ozkan, U. S. *Carbon* **2010**, *48*, 3635. (b) Choi, C. H.; Park, S. H.; Woo, S. I. *J. Mater. Chem.* **2012**, *22*, 12107.

(16) (a) Liu, H.-J.; Wang, X.-M.; Cui, W.-J.; Dou, Y.-Q.; Zhao, D.-Y.; Xia, Y.-Y. *J. Mater. Chem.* **2012**, *22*. (b) Chai, G. S.; Yoon, S. B.; Yu, J.-S. *Carbon* **2005**, *43*, 3028. (c) Chang, H.; Joo, S.; Pak, C. *J. Mater. Chem.* **2007**, *17*, 3078.

(17) (a) Yoon, S.; Chai, G.; Kang, S.; Yu, J.-S.; Gierszal, K.; Jaronec, M. *J. Am. Chem. Soc.* **2005**, *127*, 4188. (b) Yoon, S. B.; Kim, J. Y.; Kooli, F.; Lee, C. W.; Yu, J.-S. *Chem. Commun.* **2003**, *14*, 1740. (c) Kim, T.-W.; Kim, H.-D.; Jeong, K.-E.; Chae, H.-J.; Jeong, S.-Y.; Lee, C.-H.; Kim, C.-U. *Green Chem.* **2011**, *13*, 1718.

(18) Kang, S.; Chae, Y. B.; Yu, J. -S. *J. Nanosci. Nanotechnol.* **2009**, *9*, 527.

(19) Han, J. C.; Liu, A. P.; Zhu, J. Q.; Tan, M. L.; Wu, H. P. *Appl. Phys. A* **2007**, *88*, 341.

(20) Breck, D. W. *Zeolite Molecular Sieves*; John Wiley & Sons: New York, 1974; Chapter 8.

(21) Liu, N.; Song, H.; Chen, X. *J. Mater. Chem.* **2011**, *21*, 5345.